Evaluation of Pressure Bed Sensor for Automatic SAHS Screening

Guillermina Guerrero Mora, Juha M. Kortelainen, Elvia Ruth Palacios Hernández, Mirja Tenhunen, Anna Maria Bianchi, *Member, IEEE*, and Martín O. Méndez, *Member, IEEE*

I. Introduction

SLEEP apnea–hypopnea syndrome (SAHS)—with a prevalence estimated in 4% adult males and 2% adult females [1]—is the most common and dangerous condition of sleep breathing disorders. SAHS is characterized by recurrent abnormal episodes of cessation (apnea) or considerable reduction (hypopnea) of respiratory flow during sleep, which can last from a few seconds to minutes. The presence of these episodes leads oxygen desaturation (hypoxia), CO_2 retention, and sleep fragmentation. The common manifestation of suffering SAHS is excessive sleepiness, and other symptoms are depression, decreased cognitive performance, and fatigue during the day [2]. Untreated SAHS is strongly related with severe comorbidities, such as cardiovascular disease, cardiac failure, aortic dissection, and stroke [3], [4]. In addition, growing evidence suggests SAHS epidemiologic relationship to metabolic syndrome, a combination of metabolic disturbances as hypertension, insulin resistance, increased triglycerides, abdominal obesity, and low high-density lipoprotein cholesterol. This combination increases the risk of development of type-2 diabetes mellitus and cardiovascular diseases [5], [6]. Apneas and hypopneas are classified according to their cause in three different types: 1) obstructive; 2) central; and 3) mixed. Obstructive episodes appear as a result from complete or partial collapse of the upper airway, which generates an increase in the thoracic and abdominal efforts to produce airflow. The central sleep apnea arises from the reduction in central respiratory drive, and in these episodes, the respiratory movements are absent or attenuated. Mixed sleep apnea events are caused by the combination of both central and obstructive factor; the episode is initially caused by the lack of respiratory effort and continues despite the resumption of the inspiratory efforts, which indicates an upper airway obstruction.

Polysomnography (PSG) is the standard method of clinical sleep medicine for the assessment of sleep quality and sleep disorders. PSG consists of continuous and simultaneous monitoring of several physiologic parameters in a special equipped sleep laboratory. An expert technologist scores the PSG to identify the sleep stages and detect the significant sleep events. The episodes of apnea and hypopnea are detected in the airflow signal, while the information derived from electroencephalography and oxygen saturation (SpO2) provides supportive evidence, and the thoracic and abdominal respiratory efforts are used for type event classification. The events are accounted in the apnea–hypopnea index (AHI), which has been regarded as the standard indicator of disease severity, and is calculated as the number of apneas and hypopneas per hour of sleep. Current accepted criteria consider mild, moderate, and severe categories, with $5 < \text{AHI} \leq 15$, $15 < \text{AHI} \leq 30$, and $\text{AHI} > 30$ events/hour, respectively [2].

Manuscript received April 25, 2014; revised October 2, 2014; accepted October 6, 2014. Date of publication December 9, 2014; date of current version June 5, 2015. This work was supported in part by the National Council on Science and Technology (CONACYT) under Grant 175108, and in part by the Ministry of Education through CONACYT under Grant CB-180604 and Grant CB-54623. The Associate Editor coordinating the review process was Dr. Salvatore Baglio.

G. G. Mora is with the Universidad Autónoma de San Luis Potosí, San Luis Potosí 78000, México (e-mail: guile.guerrerom@gmail.com).

J. M. Kortelainen is with the Valmistustekniikka Turvallisuustekniikka Technical Research Centre of Finland, Tampere 33101, Finland (e-mail: juha.m.kortelainen@vtt.fi).

E. R. P. Hernández and M. O. Méndez are with the Facultad de Ciencias, Universidad Autónoma de San Luis Potosí, San Luis Potosí 07360, México (e-mail: epalacios@fciencias.uaslp.mx; mmendez@galia.fc.uaslp.mx).

M. Tenhunen is with the Department of Clinical Neurophysiology, Tampere University Hospital, Tampere 33521, Finland (e-mail: mirja.tenhunen@pshp.fi).

A. M. Bianchi is with the Department of Biomedical Engineering, Politecnico di Milano, Milan 20133, Italy (e-mail: annamaria.bianchi@polimi.it).

Color versions of one or more of the figures in this paper are available online.

The growing demand and the recognition of adverse effects of SAHS have encouraged researches for the development of novel methods for robust and nonintrusive measurements and to overcome drawbacks of the expensive and time-consuming PSG procedure. Simplifying the clinical practice of sleep medicine has the potentiality to enhance the feasibility of measurements in more natural environments like home monitoring. For SAHS detection, several studies have analyzed various physiological signals, such as ECG [7]–[9], oxygen saturation [10], [11], respiratory patterns [12]–[15], breath sounds [16], among others. Some studies have investigated how to increase the performance of detection, while other studies have been performed to overcome the inconvenience of PSG. As a result, different kinds of portable and wearable systems have been proposed [17]–[19], reducing the needed number of physiological signals, increasing patient comfort, and decreasing the complexity and costs of the procedure. However, most of these systems still need to be placed on the patient's body and can interfere with the normal sleep habits.

The main sources of the motor activity during a relaxed sleep are the cardiac and respiratory cycles; therefore, several noninvasive and unrestrained sensing techniques have been explored for measuring the dynamic pressing force under the sleeping subject to extract these vital signals [20]. One of the first attempts for such sleep monitoring systems is the static charge sensitive bed (originally developed in 1981) [21], which is composed of two metal plates placed in a special foam plastic mattress allowing short-term monitoring. The static charge sensitive bed has been used to assess sleep quality, partial upper airway obstruction, obstructive apnea, periodic leg movements, or just to localize individual heartbeat pulse for heart activity [22]–[25]. Recently, taking advantage of the computational tools and the rise of new sensor technologies, different approaches with capacitive or piezoelectric sensor films [26], a pressure sensor array [27], [28] or a pressure sensor embedded on an air mattress [29], [30], and even a pneumatic-tube-like sensor have been proposed [31]. Nevertheless, the analysis of these bed-based devices has been limited to detect simulated apneas [27], [29], [31] or just central apneas in a small-scale test [28]. Thus, an extended evaluation of these systems is needed to propose their clinical or home use. In addition, a disadvantage of air mattress-based devices is the requirement of calibration in each location change, which impacts their portability.

To improve the accuracy and robustness of the signal extraction, the technical research center of Finland (VTT) developed the multichannel pressure bed sensor (PBS) composed of eight polyvinylidene fluoride (PVDF) piezoelectric film sensors to measure the dynamic change of pressure under the thoracic and abdominal regions [33]. Because the PVDF film sensors are very thin and flexible, the existence of the sensor is hardly perceptible and it may not affect the sleep of the person under measurement. The multichannel pressure recordings allow the extraction of different physiological signals, such as heart interbeat interval, respiratory effort, and movement activity.

The purpose of this paper is to validate PBS as a device capable of accurately estimating the AHI. To analyze the PBS recordings, we developed an automatic algorithm for the respiratory event (RE) detection based on the measurement of the respiration motion. Then, the algorithm computes a RE index (REI), calculated as the number of REs per hour of sleep.

The full PSG includes two elastic belts to measure thoracic and abdominal breathing effort through the lungs volume changes [respiratory inductive plethysmogram (RIP)]. As these signals provide an indirect measurement of the respiration airflow in a similar way as PBS, the automated analysis was also applied to them for the comparison. Consequently, this paper evaluates the diagnostic performance of PBS, and thoracic and abdominal RIP signals in detecting various severity levels of SAHS, by comparing REI against AHI obtained by the sleep specialist through a full PSG.

II. Measurement System

A. Pressure Bed Sensor

The developed PBS includes eight PVDF piezoelectric film sensors to measure the dynamic change of pressure induced by the vital functions under the torso of the sleeping subject. PVDF films are lightweight, thin, and highly flexible, and they self-generate the electrical charge signal by the pressing or bending force. The eight sensor films are placed into four rows and two columns covering a measurement area of 64 cm $\times$ 64 cm, installed in between two foamed rubber sheets, and covered with hygienic fabrics. The final overall dimensions are 100 cm $\times$ 72 cm and 2 cm thickness when not compressed. The shielded wire leads the electrical charge signals of the sensor to the commercial IC DDC118 from Texas Instruments, which is used for the signal acquisition. This device includes current-to-voltage conversion, continuous integration, A/D conversion, and digital filtering. The integrating cycle with an exact time period provides a notch-type low-pass filtering, which was utilized to suppress the mains interferences before the A/D conversion [32]. The sensors data were digitalized at the sampling rate of 50 Hz for each measurement channel. Fig. 1 shows a picture of the PBS device, the overall structure, and individual components of the system.

B. Signal Extraction

Physiological functions such as respiration and heartbeat differ in manner of occurrence and frequency. The heart muscle motion and blood pulsation is found in the high-frequency component of the PBS signals, while the respiratory movement is found at the lower frequency band. Respiratory signal is extracted from each sensor channel using weighted averaging with 2-s-long sliding Hanning window function, corresponding approximately with a low-pass filter with a corner frequency of 0.5 Hz. The extraction of the heartbeat interval was done via spectral averaging using Fourier-transform-based *cepstrum* method [33]. Body movements cause the strongest signal components for the PBS, and are calculated as an average value between the standard deviations for each measurement channel, named in here *Activity_PBS*. The channel-wise standard deviations are calculated using a sliding raised cosine window with a length of 4 s.

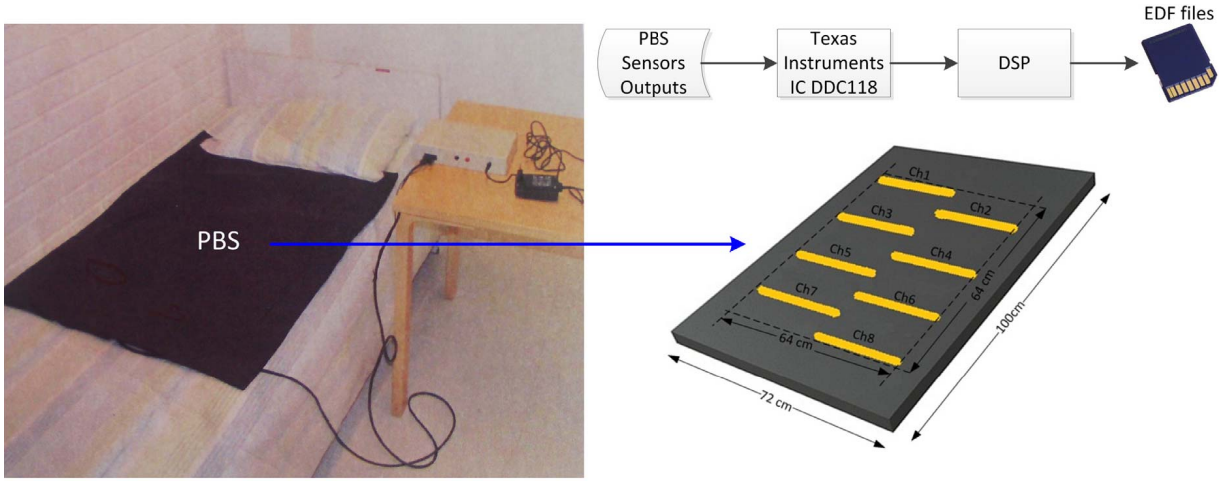

Fig. 1. Overall structure of the PBS assembly with eight PVDF sensors.

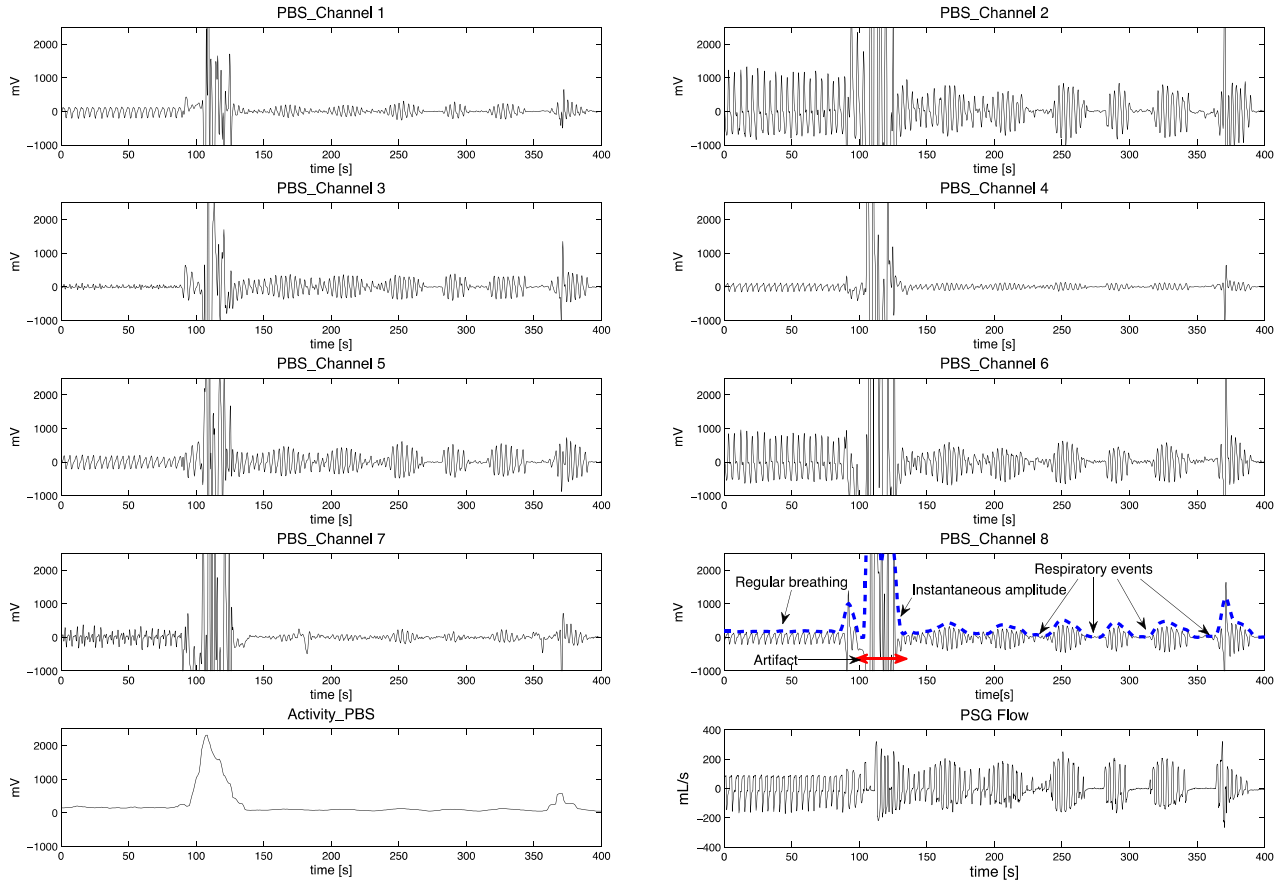

Fig. 2. Respiration signals extracted from each PBS sensor channel, the corresponding instantaneous amplitude, and the calculated Activity_PBS signal.

These algorithms are implemented on-board for a DSP, and the final recordings are written into a memory card with the European data format.

C. Signal Features

The eight channel respiration signals (PBS_channel 1, PBS_channel 2, . . . , PBS_channel 8) are obtained at different positions under the torso of the sleeping subject. The amplitude of each respiratory signal channel may vary by the location of the patient over the sensing area, by the sleeping position, and by the sleep stage. The most heavily weighted sensor exhibits a strong breathing signal, while the other sensor elements (less loaded) show a weak signal. Furthermore, more clear measurements are obtained in the supine position than in the right-/left-side position. Fig. 2 shows a data segment of the respiratory signal extracted from each PBS channel, and also the *Activity_PBS* signal. The segment initially contains a regular breathing interval, followed by an artifact caused by a

change of sleeping position, which leads to the saturation of the sensor signals and can also be localized as a maxima in the *Activity_PBS* signal. Some consecutive REs appear after the strong movement, including two hypopneas followed by four apneas. The periods of regular breathing and REs are pointed with arrows in the fourth right-hand side graph of Fig. 2. For comparison, the figure also illustrates in the lower right graph the airflow measurement (flow PSG) included in the PSG.

D. Recording Protocol and Data Set

The database comprises the recordings of a total of 24 adult patients referred to the sleep laboratory of Tampere University Hospital for suspected sleep problems. It includes 12 women and 12 men, with body mass index (BMI) of 29.33 ± 5.34 and age between 48 and 63 years. All participants underwent overnight full standard PSG study and a simultaneous recording with PBS. The PBS was placed below a foam plastic mattress with a thickness of about 12 cm and positioned under the torso of the patient. Instruments for the PSG included electrodes to measure cardiac (electrocardiogram), neuronal (electroencephalogram), and muscular (electromyogram) activity, two elastic bands for RIP on thorax and abdomen position, a pulse oximeter for oxygen saturation in blood, thermistor, and nasal cannula for airflow measurement, among others. The overnight PBS recording data and result files were written into a memory card, and are synchronized in time with the reference PSG for the analysis.

The RE scoring on the PSG signals was done through Rem-Logic software (Embla Systems limited liability company) with an automatic procedure that detects REs from the nasal airflow signal. Apneas are detected as a reduction greater or equal to 90% from the baseline for a minimum duration of 10 s. Hypopneas are scored when the nasal pressure signal deflections dropped by greater or equal to 50% and lesser than 90% of the baseline with a minimum duration of 10 s, associated with an oxygen desaturation greater or equal to 4% [34]. Classification of the apnea/hypopnea type is based on the thoracic and abdominal respiratory effort. A sleep expert examined the results and made manual corrections when necessary. The reference AHI is then calculated accounting for the total number of apneas and hypopneas divided by the total analysis time for each patient recording. The patients were clustered into four severity groups of the SAHS by the resulted AHI: 1) normal; 2) mild; 3) moderate; and 4) severe. The information of the data set is summarized in Table I, where patients are sorted for increasing order according to the AHI.

TABLE I
CLINICAL CHARACTERISTICS OF DATA SET

Severity	Patient Label	AHI [a]	BMI [b]	TAT [c]	TNE [d]
NORMAL	S1	0.12	23.2	8.40	1
	S2	0.13	21.8	7.64	1
	S3	0.23	23.6	8.74	2
	S4	0.52	32.1	9.65	5
	S5	0.72	23.9	8.34	6
	S6	1.80	25.1	7.22	13
	S7	2.55	30.9	9.04	23
	S8	3.30	27.3	8.18	27
	S9	3.49	37	6.01	21
	S10	4.02	24.2	7.46	30
	S11	4.56	29.8	8.56	39
mean	**-**	**1.94**	**27.17**	**8.11**	**15.38**
MILD	S12	5.93	24.7	5.74	34
	S13	9.76	30.9	11.17	109
	S14	12.87	27.5	7.69	99
mean	**-**	**9.52**	**27.70**	**8.19**	**80.66**
MODERATE	S15	15.01	27.3	9.66	145
	S16	17.90	29.9	9.05	162
	S17	22.00	32	7.32	161
	S18	22.92	30.7	7.02	161
	S19	27.75	40.6	6.49	180
mean	**-**	**21.11**	**32.10**	**7.90**	**161.80**
SEVERE	S20	31.74	28.4	6.18	196
	S21	41.00	27.8	8.98	368
	S22	46.97	36.3	6.79	319
	S23	50.63	34.6	8.97	454
	S24	52.21	40.6	6.61	345
mean	**-**	**41.71**	**34.71**	**7.33**	**310.33**

[a]AHI=Apnea-Hypopnea Index
[b]BMI= Body Mass Index
[c]TAT= Total Analysis Time
[d]TNE=Total Number of Events

III. SAHS DETECTION

A. Algorithm

The signals acquired by the PBS are analyzed through a developed algorithm that detects the number of REs over the recordings of one sleep night. This multichannel algorithm uses all the eight respiration signals (*PBS_channel 1, PBS_channel 2*, . . . , *PBS_channel 8*) and the activity signal (*Activity_PBS*), as described in Section II. The algorithm was designed to automatically detect decrements in the amplitude of the respiratory signal caused by SAHS events. The processing approach involves six main stages that are described first, and the selection of the parameters is given in the next section.

Stage 1: Determine the amplitude of each respiration signal from PBS. The instantaneous amplitude is calculated by means of the Hilbert transform, and smoothed with a third-order Butterworth low-pass filter with a corner frequency of 0.1 Hz (to maintain only the apnea frequency, founded in the very low frequency band [35]). Next, the obtained respiration amplitude signal is downsampled into 1 Hz with linear interpolation.

Stage 2: Remove movement artifact periods. These periods are identified via the *Activity_PBS* signal, which is initially normalized with the BMI, and then smoothed by a moving average filter with a 20-s window length. The artifacts are identified as those segments that exceed the predefined threshold. Once identified, the segments are replaced by the average respiration amplitude value of the previous and posterior 10 s.

Stage 3: Extract the dominant patterns and synthesize the information from the multiple respiratory measures coming

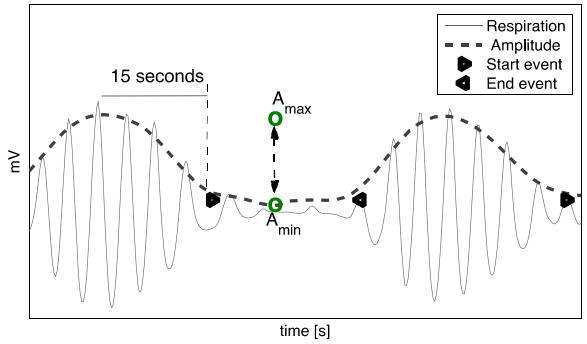

Fig. 3. Respiration signal form PBS_Channel 2 and the corresponding instantaneous amplitude.

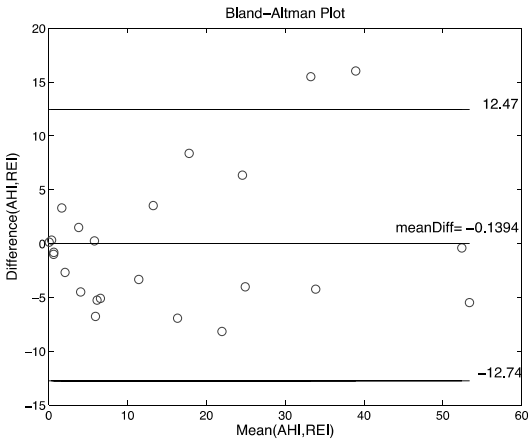

Fig. 4. Bland–Altman plot of REI from PBS_mult against AHI. The upper and lower solid black lines at 12.47 and −12.74, respectively, are the 95% limits of agreement. The middle solid black line indicates mean difference (bias) between the compared indexes. Each circle represents one subject.

from PBS. We applied principal component analysis (PCA) over the eight amplitude signals on data blocks using a sliding window of 7-min length to handle the dynamics of these time-varying multivariate data. As an average over the whole data set, the first principal component reproduces about 80% of the respiration amplitude signal variance. Exploring the information on the remaining principal components, we concluded that they do not offer valuable information for our purposes. Consequently, the respiration amplitude signal *PBS_mult* is obtained from the scores associated with the first principal component and is used for SAHS event detection.

Stage 4: Calculate the respiration amplitude baseline. Here, *PBS_mult* signal is smoothed with a sliding median filter in the forward direction, obtaining a bsl_1 signal. Then, the *PBS_mult* is reversed and median filtered to obtain a bsl_2 signal. Finally, the baseline is calculated by

$$\text{baseline}(n) = \max[\text{bsl}_1(n), \text{bsl}_2(n)] \tag{1}$$

where n is the sample number.

Stage 5 (Detect REs): A potential RE is identified when the calculated respiration amplitude PBS_mult is under the baseline signal. If within the potential event PBS_mult decreases at least below a threshold with respect to the 90% value of the previous 15 s, and is kept under this level for more than 10 s, then an RE is scored. However, if the duration of the RE reaches 120 s or more, then it is considered not valid and discarded. The decrease Amp_dec (percentage) on PBS_mult is calculated by (2), where $A_{\max}$ is the 90% of the amplitude of the 15-s preceding onset of the event and $A_{\min}$ is the minimum value found within the start and end of the event, which is illustrated in Fig. 3

$$\text{Amp\_dec} = \frac{A_{\max} - A_{\min}}{A_{\max}} \times 100\%. \tag{2}$$

Stage 6: Calculate the REI. REI is calculated for each recording as the sum of the detected RE divided by the analysis time, which is the total analysis time subtracted with the cumulated artifact periods.

B. Parameter Selection

The modifiable parameters in the algorithm are the length *wl* and the shift *dt* of the sliding window for the PCA in stage 3, the length of the window *wl_BL* for the baseline calculation, and the event reduction threshold *red_TH* in stages 4 and 5, respectively.

To select *wl* and *dt*, PCA-based algorithm was applied at different values of these parameters. For each patient and each parameter combination, the algorithm produces an amplitude signal *PBS_mult(wl, dt)*. We explore the complete data set considering the annotations scored by the expert on the PSG signals. Over each *PBS_mult*(wl, dt) signal, (2) was used to calculate the *Amp_dec* presented on each scored event.

Separated in apneas and hypopneas (a total of 1503 and 1398 events, respectively), a probability distribution of the *Amp_dec* data was calculated for each *PBS_mult* [*PD_PBS(wl, dt)*] and for also the nasal airflow signal (flow included in the PSG) as the reference (*PD_Flow*). For robustness, the leave-one-out cross validation has been applied to ensure the statistical validity. With $N = 24$ patients, the data from $N - 1$ patients are used for training to obtain a *PD_PBS* and conduct N separate operations. The events from one patient are successively left out from the training group. The correlation value (r) was calculated to quantify the strength of the linear relationship between the reference *PD_Flow* and each *PD_PBS*. To obtain an overall assessment, the values of r are averaged. The final parameter selection—$wl = 7$ min, updated each minute ($dt = 1$ min)—is done by searching the maximum median r and prioritizing the hypopnea events since the PBS sensor presents a lower sensitivity during these events.

To simultaneously select *red_TH* and *wl_BL*, using the baseline calculated with *wl_BL* set at 10 to 300 s in nonequidistant steps, the REI was obtained through an RE detection using *red_TH*, which varies from 2% to 90% in steps of 2%. Once again, leave-one-patient-out cross-validation procedure is carried out for the 24 recordings. The correlation coefficient between REI and AHI is calculated and averaged to produce the mean performance. The (*wl_Bl, red_TH*) pair values producing the highest mean performance was 30 s associated with a percent decrease of 44%. The same analysis is applied for RIP signals, resulting in *red_TH* equal to 48% and *wl_Bl* equal to 30 s for both thorax and abdomen signals.

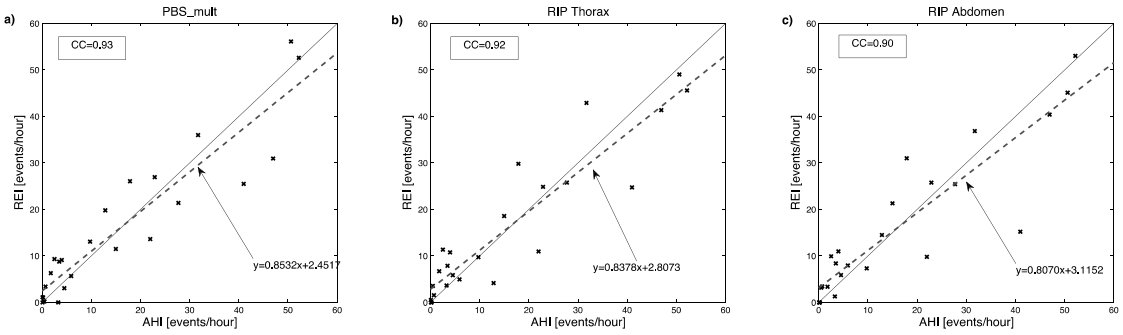

Fig. 5. Scatter plots of the reference AHI compared with REI scored on (a) PBS_mult signal, (b) thoracic effort signal, and (c) abdominal effort signal.

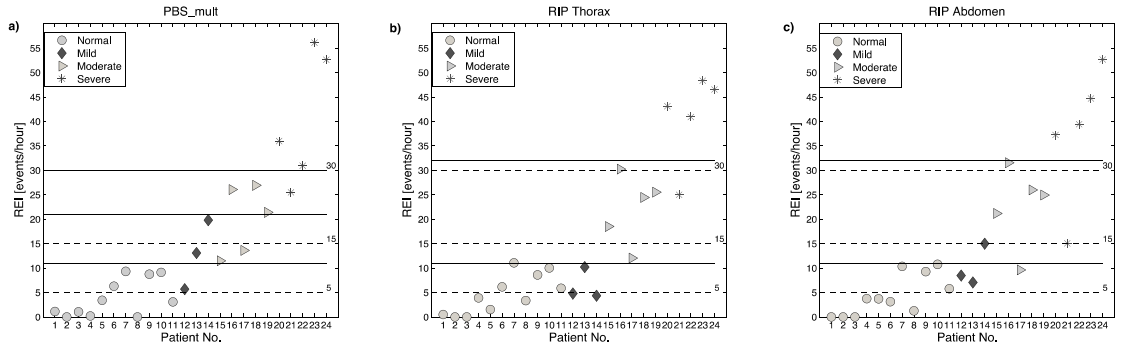

Fig. 6. Severity group classification through the REI from (a) PBS_mult signal, (b) thoracic effort signal, and (c) abdominal effort signal.

IV. Results

The set of signals obtained from the PBS for each of the 24 patients is tested through the developed amplitude-based algorithm with the selected parameters. The same algorithm is applied to the thoracic and abdominal RIP signals of the respiratory effort, provided by the PSG, to compare against the performance of the proposed PBS device. The obtained REI is compared in several ways with the reference AHI (from the PSG manual scoring). The Bland–Altman plot used to assess the agreement between REI from PBS and AHI is shown in Fig. 4. The plot indicates the difference between each REI and the corresponding AHI. The mean difference of the indexes was almost zero, and the 95% of the number of events differences were between -12.74 and 12.47 events/hour, the confidential interval of mean difference. There is a good agreement across a wide range of SAHS severity except in two cases, where PBS underestimated the AHI by 16.88 and 14.25 events/hour.

The overall relationship of REI in relation to the AHI for the analyzed signals is shown in the scatter plot of Fig. 5, in which each point represents the REI of one patient; the solid line is the identity line, and the dashed line corresponds to the regression model. The graph in Fig. 5(a) shows the REI from *PBS_mult* signal. The middle and right graphs [Fig. 5(b) and (c)] show the REI from thoracic and abdominal effort signals versus the reference. A better linear relation is observed for *PBS_mult* with $r = 093$ than for RIP signals with $r = 092$ and $r = 090$, for the thorax and abdomen, respectively.

As shown in Table I, patients are grouped through AHI into severity categories of SAHS: normal (AHI $<$ 5) with 11 patients, mild ($5 \geq$ AHI $>$ 15) with three patients, moderate ($15 \geq$ AHI $>$ 30) with five patients, and severe (AHI $\geq$ 30) with five patients. Evaluating REI as severity indicator of SAHS, the Cohen's kappa coefficient (κ) is used to quantifying the intraclass agreement between REI and AHI, and the results are shown in Table III. For PBS, using official ratings (5, 15, and 30), $k = 069$ is obtained, indicating a good agreement. However, considering the bias presented for this surrogate signal (Fig. 5) adequate severity ratings need to be established. Considering 11, 20, and 30 events/hour (almost twice the bias), REI shows a kappa value equal to 0.76 which is an improvement in the results. Fig. 6 shows the REI obtained for each patient; the dashed lines at 5, 15, and 30 events/hour denote the official thresholds established in the mentioned severity criteria. The solid black lines are the new thresholds of events per hour established for each the indirect measures. In Fig. 6(a), the REI obtained from PBS for each patient, and in Fig. 6(b) and (c), the REI obtained from thoracic and abdominal RIP respiratory effort. Different markers were used to identify the patient into the corresponding severity category according to the information in Table I. We can observe that using REI, it is difficult to find difference between mild and moderate groups; then, by merging these middlemost categories to have normal, mild-moderate, and severe groups, the corresponding kappa coefficient improves to $k = 086$. A similar evaluation is applied for the RIP signals with the results shown in Table II. In Fig. 6, for RIP signals, it is possible to observe a complete overlap between normal and mild categories, which indicates that the correct separation between these categories is not possible. By setting appropriated category ratings to 11 and 32, the kappa coefficient for both thorax and abdomen signals is $k = 073$ for the three categories: 1) normal-mild; 2) moderate;

TABLE II
KAPPA INDEX FROM THE DIFFERENT SIGNALS FOR THE ANALYZED CASES

κ	*PBS_mult*	RIP thorax	RIP abdomen
Case1: REI=[5 15 30]	0.56	0.39	0.39
Case 2: REI=[11 21 30]	0.75	-	-
Case 3: REI=[11 30]/[12 32] [a]	0.86	0.73	0.73

[a] REI for PBS and RIP signals respectively

TABLE III
SENSITIVITY, SPECIFICITY, AND ACCURACY FOR NORMAL AND PATHOLOGICAL IDENTIFICATION

Index	Normal/Pathologic	
	PBS_mult REI>11	thorax/abdomen REI>12
Sensitivity [%]	100	100/93
Specificity [%]	92	90/90
Accuracy [%]	96	96/92

and 3) severe. Summarizing (Table II), three cases are analyzed: using the official ratings to separate between four categories, modifying the official by appropriated ratings to separate between four categories, and finally modifying the official by appropriated ratings to separate three categories.

Finally, the diagnostic ability of the REI to detect normal and pathological subjects is evaluated in terms of sensitivity, specificity, and accuracy. As shown in Table III, *PBS_mult* signal presents a sensitivity of 100%, a specificity of 92%, and an accuracy of 96%. For the thorax RIP signal, the results are 100%, 90%, and 96%, respectively, while for the abdomen RIP signal, the same indexes show 93%, 90%, and 92%.

V. CONCLUSION

This paper evaluates the performance in SAHS detection of a totally unobtrusive PBS system designed for sleep monitoring. The PBS uses PVDF films, which are very sensitive, thin, and flexible, thus the existence of the sensors is hardly perceptible for the patient under measurement, and it may not affect the sleep process. The performance of PBS is compared with reference methods, the gold standard of PSG manual scoring, and automatic detection from the RIP bands. With the implemented algorithm that automatically detects REs, the severity SAHS indicator REI is obtained. Our main observations are as follows: 1) PBS signals convey useful information for SAHS detection in an unobtrusive way and 2) thorax, abdominal, and PBS signals have similar performance for SAHS detection.

One of the main advantages of PBS is the ability to obtain three relevant physiological signals from one device: 1) respiratory effort; 2) heart rate; and 3) movement activity. Thus, PBS could be used to evaluate different sleep pathologies, such as SAHS, insomnia, periodic leg movement, and cardiac dysfunctions. The proposed analysis is only based on the respiratory effort in association with the activity signal. It is reported that heart rate also contains useful information for SAHS detection [7]–[9], and a multivariable analysis could be done for improved results. In addition, due to the multichannel nature of PBS, different information can be computed, for example, the body position and weight. Although the respiratory inductive plethysmography is a widely accepted method for qualitative noninvasive respiratory measurement [36], [37], PBS can offer a noninvasive and unobtrusive way to obtain similar measures without the need of contact sensors. This feature of PBS allows an evaluation in a more comfortable way and within a daily environment.

The obtained results for this data set are comparable with the previous studies presented by several research groups using direct or indirect airflow measurement. Varady *et al*. [12] proposed an automated method for the detection of the presence or the absence of normal breathing based on the direct airflow measurement from PSG records. Their algorithm produced an average detection performance of over 90%. Han *et al.* [15] presented a similar approach for the detection of obstructive apneas, and the overall agreement rate was 92.0% ($\kappa = 0.78$). In another way, Yadollahi and Moussavi [16] used tracheal breathing sounds and the blood oxygen saturation level; the results show a correlation of 96% with PSG. Some of these investigations detect just the apnea index, but the hypopneas have the same clinical consequence and they should be considered (as in this paper) to determine the SAHS severity. Furthermore, PBS shows better performance compared with the results presented for thoracic and abdominal RIP respiratory signal.

A similar device to PBS is described in [28], which proposes the validation of a pressure sensor array for the screening of central apneas; with six patients, the found kappa value was 0.75, and the sensitivity and specificity were 87.6% and 99.9%, respectively. For those sensitive mattress devices, central apneas are easily detected due the total lack of respiratory movements in contrast to obstructive apneas (the most common type of apnea), where the transducers detect the persistent respiratory effort. On the other hand, Shin *et al.* [31] used a sensitive air mattress for the detection of simulated sleep apnea events and found a sensitivity and positive predictive value of 93% and 88%, respectively. It is important to note that in this paper, we do not make distinction between apneas and hypopneas, and even between different apnea types. We explored PBS as a tool to indicate the presence and severity of sleep breathing disorders. However, the information of the type of the event (and consequently the cause) is important to determine to define the possible treatment of the patient.

In clinics, the percentage reduction in the nasal airflow signal is 50% for hypopneas and 90%–100% for apneas. However, those values should be taken as tunable factors for the surrogate signals coming from PBS and RIP. For PBS, the optimal value is 44%, while for RIP signals, it is 48% to detect both hypopneas and apneas. In addition, severity ratings are also modified to compensate the bias due to different

sources. For example, for the respiratory scoring based on the PSG signals, the oxygen desaturation is used to validate hypopnea events. Herein, the event detection is based only on the respiratory measurement, and if such validation is not included, then some false events can be detected. With this, PBS shows a high accuracy in separate normal and pathological subjects.

The proposed device enables portable recording at home, providing a support tool especially for those patients with limited mobility, or critical illness. According to the guidelines of Task Force of Unattended Portable Monitors for sleep disordered breathing [38], the current system would belong to type 4, since only one signal type is measured. It must fulfill some of the basic concerns dictated by the Task Force, such as safety, easy use, reliability, durability, economy, and diagnosis accuracy.

Finally, the main limitation of this paper is the small data set that contains a high number of normal subjects with a reduced number in the light and moderate categories. Thus, a large data set is needed to validate the system for clinical purposes. In addition, the study is focused on a general SAHS index that includes all types of apneas, and further study is needed to evaluate the possibility of differentiate among apnea types. The developed algorithm uses PCA to compose information for the respiratory effort from multiple movement signals and as such the method is applicable to a multichannel sensor assembly only. Even with the limitations, the results suggest that the method could be used as pretest or posttest tool for SAHS evaluation. In conclusion, PBS could be a noninvasive and unobtrusive promise for home monitoring and clinical support in SAHS diagnosis.

REFERENCES

[1] T. Young, P. E. Peppard, and D. J. Gottlieb, "Epidemiology of obstructive sleep apnea: A population health perspective," *Amer. J. Respirat. Critical Care Med.*, vol. 165, no. 9, pp. 1217–1239, 2002.

[2] The report of an American Academy of Sleep Medicine task force, "Sleep-related breathing disorders in adults: Recommendations for syndrome definition and measurement techniques in clinical research," *Sleep*, vol. 22, no. 5, pp. 667–689, 1999.

[3] T. Douglas and J. S. Floras, "Sleep apnea and heart failure: Part I: Obstructive sleep apnea," *Circulation*, vol. 107, no. 12, pp. 1671–1678, 2003.

[4] K. Narkiewicz, N. Montano, C. Cogliati, P. J. van de Borne, M. E. Dyken, and V. K. Somers, "Altered cardiovascular variability in obstructive sleep apnea," *Circulation*, vol. 98, no. 11, pp. 1071–1077, 1998.

[5] A. D. Calvin, F. N. Albuquerque, F. Lopez-Jimenez, and V. K. Somers, "Obstructive sleep apnea, inflammation, and the metabolic syndrome," *Metabolic Syndrome Rel. Disorders*, vol. 7, no. 4, pp. 271–277, 2009.

[6] M. S. Ip, B. Lam, M. M. Ng, W. K. Lam, K. W. Tsang, and K. S. Lam, "Obstructive sleep apnea is independently associated with insulin resistance," *Amer. J. Respirat. Critical Care Med.*, vol. 165, no. 5, pp. 670–676, 2002.

[7] T. Penzel, J. McNames, P. de Chazal, B. Raymond, A. Murray, and G. Moody, "Systematic comparison of different algorithms for apnoea detection based on electrocardiogram recordings," *Med. Biol. Eng. Comput.*, vol. 40, no. 4, pp. 402–407, 2002.

[8] P. de Chazal, C. Heneghan, E. Sheridan, R. Reilly, P. Nolan, and M. O'Malley, "Automated processing of the single-lead electrocardiogram for the detection of obstructive sleep apnoea," *IEEE Trans. Biomed. Eng.*, vol. 50, no. 6, pp. 686–696, Jun. 2003.

[9] M. O. Méndez *et al.*, "Automatic screening of obstructive sleep apnea from the ECG based on empirical mode decomposition and wavelet analysis," *Physiol. Meas.*, vol. 31, no. 3, p. 273, 2010.

[10] J. V. Marcos, R. Hornero, D. Álvarez, M. Aboy, and F. del Campo, "Automated prediction of the apnea-hypopnea index from nocturnal oximetry recordings," *IEEE Trans. Biomed. Eng.*, vol. 59, no. 1, pp. 141–149, Jan. 2012.

[11] B. H. Taha *et al.*, "Automated detection and classification of sleep-disordered breathing from conventional polysomnography data," *Sleep*, vol. 20, no. 11, pp. 991–1001, 1997.

[12] P. Varady, T. Micsik, S. Benedek, and Z. Benyo, "A novel method for the detection of apnea and hypopnea events in respiration signals," *IEEE Trans. Biomed. Eng.*, vol. 49, no. 9, pp. 936–942, Sep. 2002.

[13] H. Nakano, T. Tanigawa, T. Furukawa, and S. Nishima, "Automatic detection of sleep-disordered breathing from a single-channel airflow record," *Eur. Respirat. J.*, vol. 29, no. 4, pp. 728–736, 2007.

[14] S. S. Grover and S. D. Pittman, "Automated detection of sleep disordered breathing using a nasal pressure monitoring device," *Sleep Breathing*, vol. 12, no. 4, pp. 339–345, 2008.

[15] J. Han, H. B. Shin, D.-U. Jeong, and K. S. Park, "Detection of apneic events from single channel nasal airflow using 2nd derivative method," *Comput. Methods Programs Biomed.*, vol. 91, no. 3, pp. 199–207, 2008.

[16] A. Yadollahi and Z. Moussavi, "Acoustic obstructive sleep apnea detection," in *Proc. Annu. Int. Conf. IEEE EMBS*, Sep. 2009, pp. 7110–7113.

[17] C. Heneghan *et al.*, "A portable automated assessment tool for sleep apnea using a combined Holter-oximeter," *Sleep*, vol. 31, no. 10, pp. 1432–1439, 2008.

[18] S. Park and S. Jayaraman, "Enhancing the quality of life through wearable technology," *IEEE Trans. Biomed. Eng.*, vol. 22, no. 3, pp. 41–48, May/Jun. 2003.

[19] U. Anliker *et al.*, "AMON: A wearable multiparameter medical monitoring and alert system," *IEEE Trans. Inf. Technol. Biomed.*, vol. 8, no. 4, pp. 415–427, Dec. 2004.

[20] J. Alihanka, *Sleep Movements and Associated Autonomic Nervous Activities in Young Male Adults*. Turku, Finland: Univ. Turku, 1982.

[21] J. Alihanka, K. Vaahtoranta, and I. Saarikivi, "A new method for long-term monitoring of the ballistocardiogram, heart rate, and respiration," *Amer. J. Physiol.-Regulatory, Integr. Compar. Physiol.*, vol. 240, no. 5, pp. R384–R392, 1981.

[22] M. Partinen, J. Alihanka, and J. Hasan, "Detection of sleep apneas by the static charge sensitive bed," in *6th Eur. Congr. Sleep Res.*, Zurich, Switzerland, Mar. 1982.

[23] O. Polo, L. Brissaud, B. Sales, A. Besset, and M. Billiard, "The validity of the static charge sensitive bed in detecting obstructive sleep apnoeas," *Eur. Respirat. J.*, vol. 1, no. 4, pp. 330–336, 1988.

[24] T. Salmi, T. Telakivi, and M. Partinen, "Evaluation of automatic analysis of SCSB, airflow and oxygen saturation signals in patients with sleep related apneas," *Chest*, vol. 96, no. 2, pp. 255–261, 1989.

[25] T. Salmi, M. Partinen, M. Hyyppä, and E. Kronholm, "Automatic analysis of static charge sensitive bed (SCSB) recordings in the evaluation of sleep-related apneas," *Acta Neurol. Scandin.*, vol. 74, no. 5, pp. 360–364, 1986.

[26] J. M. Kelly, R. E. Strecker, and M. T. Bianchi, "Recent developments in home sleep-monitoring devices," *ISRN Neurol.*, vol. 2012, Sep. 2012, Art. ID 768794.

[27] D. Townsend, M. Holtzman, R. Goubran, M. Frize, and F. Knoefel, "Relative thresholding with under-mattress pressure sensors to detect central apnea," *IEEE Trans. Instrum. Meas.*, vol. 60, no. 10, pp. 3281–3289, Oct. 2011.

[28] D. Townsend, R. Goubran, F. Knoefel, and J. Leech, "Validation of unobtrusive pressure sensor array for central sleep apnea screening," *IEEE Trans. Instrum. Meas.*, vol. 61, no. 7, pp. 1857–1865, Jul. 2012.

[29] K. Watanabe, T. Watanabe, H. Watanabe, H. Ando, T. Ishikawa, and K. Kobayashi, "Noninvasive measurement of heartbeat, respiration, snoring and body movements of a subject in bed via a pneumatic method," *IEEE Trans. Biomed. Eng.*, vol. 52, no. 12, pp. 2100–2107, Dec. 2005.

[30] P. Chow, G. Nagendra, J. Abisheganaden, and Y. T. Wang, "Respiratory monitoring using an air-mattress system," *Physiol. Meas.*, vol. 21, no. 3, pp. 345–354, 2000.

[31] J. H. Shin, Y. J. Chee, D.-U. Jeong, and K. S. Park, "Nonconstrained sleep monitoring system and algorithms using air-mattress with balancing tube method," *IEEE Trans. Inf. Technol. Biomed.*, vol. 14, no. 1, pp. 147–156, Jan. 2010.

[32] J. M. Kortelainen and J. Virkkala, "FFT averaging of multichannel BCG signals from bed mattress sensor to improve estimation of heart beat interval," in *Proc. 29th Annu. Int. Conf. IEEE EMBS*, Aug. 2007, pp. 6685–6688.

[33] J. M. Kortelainen, M. van Gils, and J. Parkka, "Multichannel bed pressure sensor for sleep monitoring," in *Proc. Comput. Cardiol. (CinC)*, Sep. 2012, pp. 313–316.

[34] C. Iber, S. Ancoli-Israel, A. Chesson, and S. Quan, *The AASM Manual for the Scoring of Sleep and Associated Events: Rules, Terminology and Technical Specifications*. Darien, IL, USA: American Academy of Sleep Medicine, 2007.

[35] M. O. Méndez *et al.*, "Detection of sleep apnea from surface ECG based on features extracted by an autoregressive model," in *Proc. 29th Annu. Int. Conf. IEEE EMBS*, Aug. 2007, pp. 6105–6108.

[36] A. Eberhard, P. Calabrese, P. Baconnier, and G. Benchetrit, "Comparison between the respiratory inductance plethysmography signal derivative and the airflow signal," in *Frontiers in Modeling and Control of Breathing*. Berlin, Germany: Springer-Verlag, 2001, pp. 489–494.

[37] R. T. Brouillette, A. S. Morrow, D. E. Weese-Mayer, and C. E. Hunt, "Comparison of respiratory inductive plethysmography and thoracic impedance for apnea monitoring," *J. Pediatrics*, vol. 111, no. 3, pp. 377–383, 1987.

[38] N. A. Collop *et al.*, "Clinical guidelines for the use of unattended portable monitors in the diagnosis of obstructive sleep apnea in adult patients," *J. Clin. Sleep Med.*, vol. 3, no. 7, pp. 737–747, 2007.